PAPER • OPEN ACCESS

A computational inversion method for interference suppression in reconfigurable thinned ring arrays

View the article online for updates and enhancements.

A computational inversion method for interference suppression in reconfigurable thinned ring arrays

Federico Boulos [1], Luca Dall'Asta [1], Giorgio Gottardi [1], Mohammad Abdul Hannan [1], Alessandro Polo [1], Aaron Salas-Sanchez [1,2], and Marco Salucci [1]

[1] ELEDIA Research Center (ELEDIA@UniTN - University of Trento), I-38123 Trento, Italy
[2] Department of Applied Physics, University of Santiago de Compostela, Santiago de Compostela, 15705, Spain

E-mail: `marco.salucci@unitn.it`

Abstract. An inversion strategy for dynamically thinning (i.e., turning on and off) the radiating elements of ring arrays in order to maximize the signal-to-noise ratio is presented. Since thinned arrays provide only average sidelobe performances, but the directions of arrival (DoAs) of interferences can be arbitrary, a set of thinning configurations that guarantee a sufficient interference rejection in the whole angular region outside the main lobe is off-line selected. The on-off status of the array elements is then dynamically switched among such pre-computed thinning sequences until the one providing the best signal-to-interference performance is identified. A set of numerical results is reported and discussed to assess the effectiveness and potentialities as well as current limitations of the dynamic thinning approach in dealing with interference suppression of ring arrays.

1. Introduction

Array thinning has been widely used in the design of antenna arrays to reduce the level of the secondary lobes when using isophoric excitations [1]-[3]. Starting from a full configuration with array elements disposed on a regular lattice, thinned arrangements are obtained by turning off or removing a sub-set of elements to synthesize a density taper over the aperture aimed at generating low sidelobes, while keeping the width of the main lobe close to that of the corresponding fully-populated array. Thanks to these advantages, thinned arrays are generally adopted to simplify the antenna architecture and have beam-forming networks (BFNs) with high power efficiencies since controllable amplifiers are avoided.

The problem of designing thinned arrays has been studied for decades and a wide number of synthesis techniques have been proposed [4]-[7]. Originally, design approaches devoted to reproduce the current taper of reference continuous apertures generating patterns with low secondary lobes have been introduced [4] by statistically placing more/less array elements where the current amplitude of the reference distribution is higher/lower.

Thanks to the enhanced computation capabilities of modern computers, thinned arrays has been also recently synthesized through optimization algorithms able to easily handle complex array geometries and constraints. Genetic Algorithms (GAs) have been firstly used [5], while later global optimizers based on swarm intelligence, like the Ant Colony Optimization (ACO) [6] and the Particle Swarm Optimization (PSO) [7], have been exploited, as well. Although effective, the

main limitation of these techniques is the computational burden necessary to reach convergence especially when large number of array elements is at hand.

Besides the synthesis strategy, another key-issue of thinned arrays is related to the radiated static pattern that prevents their application to radars or communications since the time-varying DoAs of undesired signals impinging on the antenna can produce an incorrect reception of the desired one drastically reducing the quality of service. To avoid such a problem still maintaining the simplicity of thinned architectures, dynamic [8] and adaptive [9] strategies have been proposed. Dealing with linear arrangements, radio-frequency (RF) switches have been added to the control points of a fully-populated array to connected or disconnect the array elements from the BFN and change the thinning sequence of the array. In the former approach [8], a finite set of thinning sequences has been computed off-line and then used to change the on-off status of the array elements until a sufficient quality of the desired signal was achieved. Differently, the problem at hand has been formulated as an optimization one in [9] where the objective is the maximization of the signal-to-noise-plus-interference ratio ($SINR$) in case the direction of arrival of the desired signal in known or, otherwise, the minimization of the antenna output power.

Despite the sub-optimal interference rejection performances, dynamic solution generally provides a faster reaction-time to the changes of the quality of the received signal even though switching among a limited set of pre-computed on-off configurations. Therefore, it seems to be more suitable for the control of reconfigurable planar thinned arrays where the dimension of the solution space (i.e., the number of array elements to be controlled) is larger than the linear case. This work is then devoted to analyze the performance of dynamic thinning in case of planar arrays with elements located on concentric rings. Like in [8], the thinning sequences are selected such that the corresponding power patterns provide suitable sidelobe suppression along all directions outside the main beam, while keeping constant the directivity (i.e., avoiding undesired amplitude fluctuations of the main lobe peak) in order to faithfully receive the desired signal.

2. Mathematical Formulation

Let us consider a planar array of N elements located on R concentric rings of radius $\rho_r = (r-1)\,d$, $r = 1, ..., R$, d being the radial distance between two adjacent rings. By assuming each ring composed of M_r elements such that $\sum_{r=1}^{R} M_r = N$ and the elements being uniformly-spaced along the circles [Fig. 1(a)], the location of each array element turns out being

$$
\begin{aligned}
x_{m_r} &= \rho_r \cos\left[(m_r - 1)\,\frac{2\pi}{M_r}\right] \\
y_{m_r} &= \rho_r \sin\left[(m_r - 1)\,\frac{2\pi}{M_r}\right] \\
& r = 1, ..., R;\ m_r = 1, ..., M_r\,.
\end{aligned}
\tag{1}
$$

The arising array factor turns out to be [2]

$$
AF(\theta, \phi) = \sum_{r=1}^{R} \sum_{m_r}^{M_r} a_{m_r}^{(t)} e^{j[k(x_{m_r}\sin\theta\cos\phi + y_{m_r}\sin\theta\sin\phi) + \varphi_{m_r}]}
\tag{2}
$$

where $j = \sqrt{-1}$, $k = \frac{2\pi}{\lambda}$, λ being the free-space wavelength, and (θ, ϕ) is the angular direction. Moreover, $\{a_{m_r}^{(t)};\ r = 1, ..., R,\ m = 1, ..., M_r\}$ is the set of amplitude coefficients of the t-th array control configuration, while φ_{m_r}, $r = 1, ..., R$, $m = 1, ..., M_r$ are the phase weights used for beam steering.
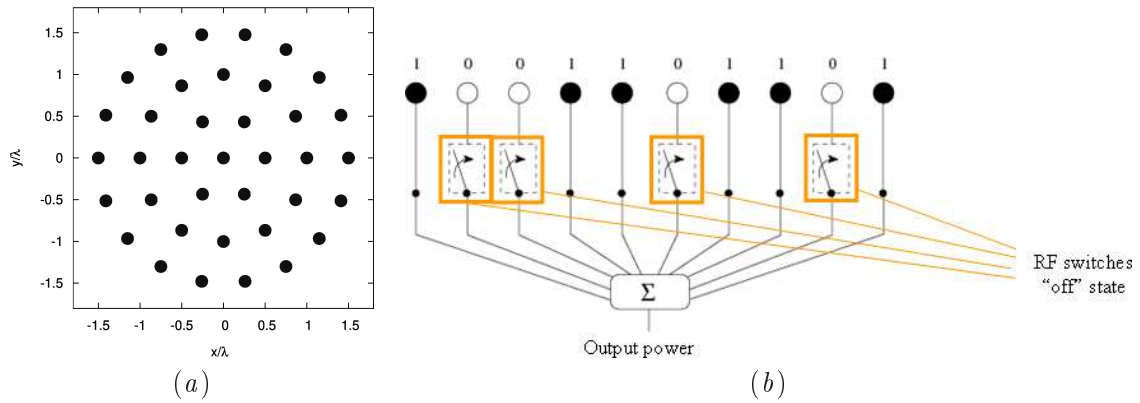
Figure 1. (a) Geometrical disposition of the array elements and (b) architecture of the beam forming network.

In (2), the time-varying amplitude coefficients are binary variables, $a_{m_r}^{(t)} = \{0, 1\}$, when $a_{m_r}^{(t)} = 1$, the corresponding m_r-th array element is in the "on" state and it is connected to the BFN to contribute to the received/transmitted signal. Otherwise ($a_{m_r}^{(t)} = 0$), the m_r-th array element is connected to a matched load and it is in the "off" state [Fig. 1(b)]. At each time instant, the antenna behaves like a thinned array [1][2] and it generates a static radiation pattern with fixed regions and levels of the sidelobes. In order to efficiently suppress an arriving interference in whatever angular direction outside the main lobe, $(\underline{\theta}, \underline{\phi}) \in \Omega$, it is not possible to use a single thinning configuration since thinned arrays only guarantee an average value of the secondary lobes across the whole secondary lobe region equal to $avg\left\{SLL^{(t)}\right\} = \frac{1}{N_{on}^{(t)}}$ [10], where $N_{on}^{(t)} = \sum_{r=1}^{R} \sum_{m_r}^{M_r} a_{m_r}^{(t)}$ is the number of active elements for the t-th array state. Different thinning configurations are then needed to suppress unwanted signals impinging on the sidelobe region. Accordingly, the interference suppression problem is formulated as follows:

Determine the minimum number, T, of thinning configurations of the array elements, $\underline{a}^{(t)} = \{a_{m_r} : r = 1, ..., R; m_r = 1, ..., M_r\}$, $t = 1, ..., T$, such that at least one allows to generate a sidelobe along the angular DoA of the interferences with level SLL_{th} below the peak of the main lobe.

Towards this end, a wider set W ($W > T$) of trial thinning configurations, $\{\underline{a}^{(w)}; w = 1, ..., W\}$, fitting user-defined constraints (e.g., minimum peak directivity D_{max}, $D_{max} \propto N_{on}^{(w)}$, $N_{on}^{(w)}$ being the number of active elements of the w-th excitation set) is generated. For each w-th thinned array, the angular directions (denoted as "nulling directions") where the power pattern satisfy the following condition (Fig. 2)

$$\left|AF^{(w)}(\theta, \phi)\right|^2 < SLL_{th} \tag{3}$$

are listed in a vector $(\underline{\theta}, \underline{\phi})^{(w)}$.

Then, the W thinning configurations are sorted according to the number of directions in each $(\underline{\theta}, \underline{\phi})^{(w)}$ vector, $w = 1, ..., W$. The minimum number of T on-off sequences, $\{\underline{a}^{(t)}, t = 1, ..., T\}$ such that

$$\bigcup_{t=1}^{T} (\underline{\theta}, \underline{\phi})^{(t)} = \Omega \tag{4}$$
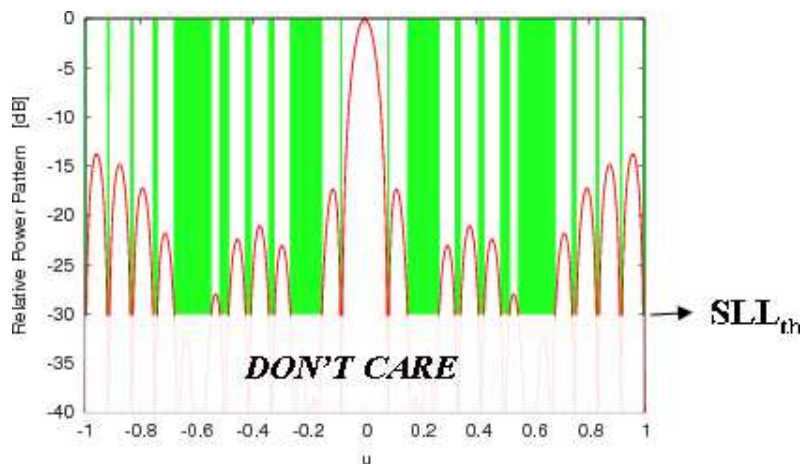
Figure 2. Graphical representation of the nulling region.

are selected according to the procedure proposed in [8] and stored in a look-up table. During the real-time operations when the $SINR$ value turns out to be smaller than pre-determined threshold, $SINR_{th}$, the working thinning configuration is automatically updated to the sequence among the T off-line defined $(\underline{a}^{(t)} \to \underline{a}^{(t+1)}; t = 1, ..., T-1$ or $\underline{a}^{(T)} \to \underline{a}^{(1)})$ that restore the correct functioning of the system $(SINR\left\{\underline{a}^{(t)}\right\} > SINR_{th})$.

3. Numerical Results

This section is devoted to assess the dynamic thinning strategy as applied to rings arrays through a set of representative numerical examples. As a benchmark, an array with $N = 19$ elements displaced over two concentric rings plus and additional element at the array center (i.e., $R = 3$) has been considered. The distance between the array rings has been set to $d = \frac{\lambda}{2}$, while the number of elements on the two outer rings amounts to $M_2 = 6$ and $M_3 = 12$, respectively.

In the first example (*Example 1*), the number of active elements for each thinning configuration has been set to $N_{on}^{(t)} = 17$, $t = 1, ..., T$ to have 90% of elements on (i.e., a reduction of the aperture efficiency of 10%) [2][10]. By setting the minimum interference rejection level to the value $SLL_{th} = -20dB$, the number of pre-computed on-off sequences, determined according to (4), turned out equal to $T = 8$. For illustrative purposes, a representative subset of the $T = 8$ thinned arrays is given in Fig. 3 where the on-off configurations of the array element are shown (Fig. 3 - *left column*), the active elements being reported with a black circle, along with the corresponding radiated power patterns (Fig. 3 - *central column*).

Moreover, the sidelobe suppression performance of the first t thinning sequences are also reported in Fig. 3 (*right column*) in terms of the binary interference suppression function $Q\left(\underline{\theta}, \underline{\phi}\right)$ $[Q\left(\underline{\theta}, \underline{\phi}\right) = 1$ if $\exists t \in [1, T]$ such that $\left|AF^{(t)}\left(\theta, \phi\right)\right|^2 < SLL_{th}$, $Q\left(\underline{\theta}, \underline{\phi}\right) = 0$ otherwise].

In this example, the thinned array arrangement providing the widest interference-suppression capability (Fig. 3 - $t = 1$) generates a secondary lobe lower than SLL_{th} for more than 75% of the sidelobe region. By using the first $T = 2$ thinning configurations (i.e., $t = 1$ and $t = 2$ - Fig. 3), this latter percentage grows up to 95% (Fig. 3 - $t = 2$, *right column*). The second example (*Example 2*) deals with a sidelobe threshold reduced down to $SLL_{th} = -30dB$, while the aperture efficiency has been set to 80% (i.e., $N_{on}^{(t)} = 15$, $t = 1, ..., T$) to increase the number of "admissible" on-off sequences [8]. Because of the more stringent requirement on the sidelobes, $T = 24$ different thinning configurations has been needed. A subset of the thinned arrays, power patterns, and suppression indexes are given in Fig. 4. The thinning sequence enabling the widest
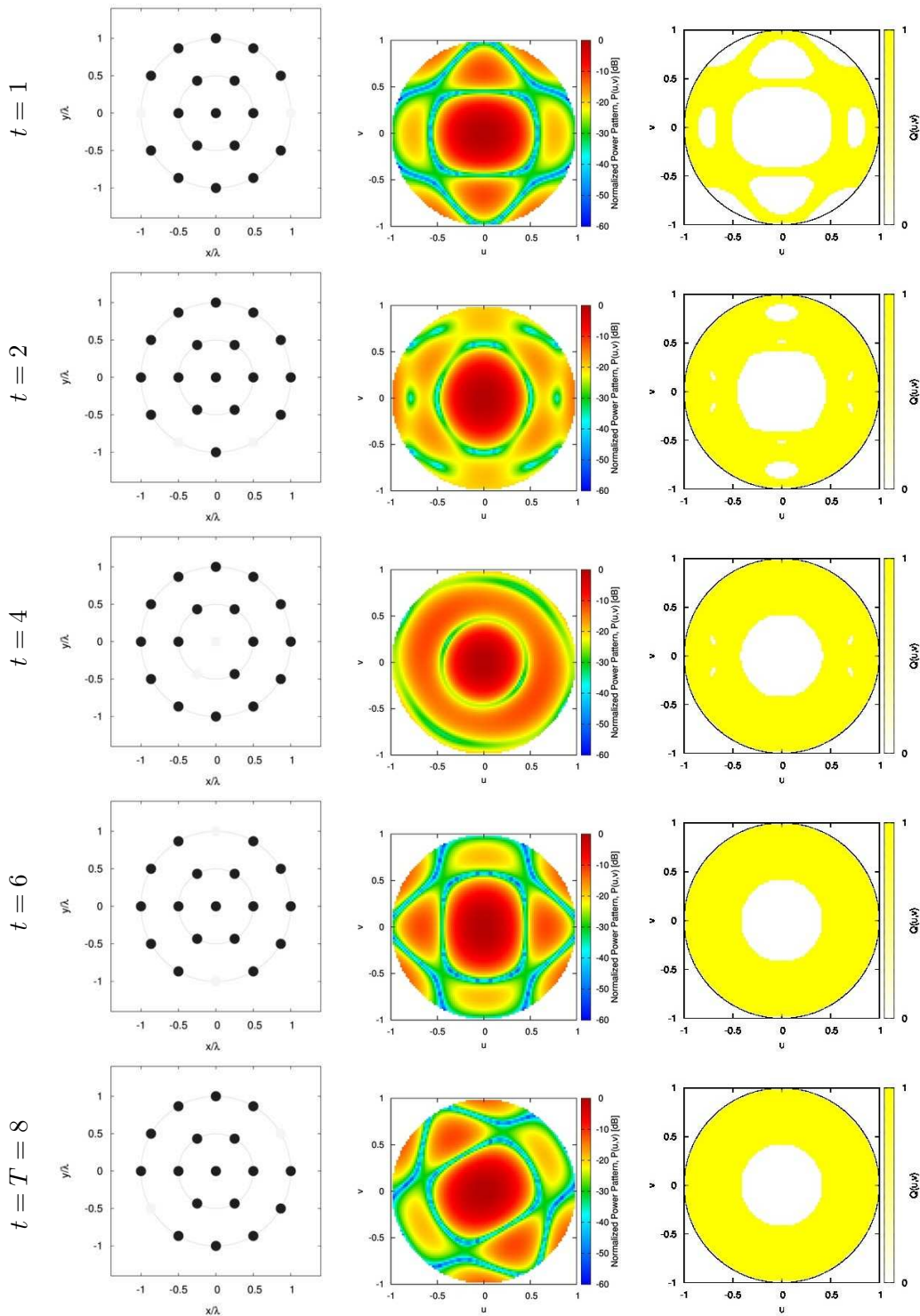
Figure 3. *Example 1* - $[N = 19, d = \frac{\lambda}{2}, N_{on}^{(t)} = 17, SLL_{th} = -20dB]$ - Set of thinning arrays (*left column*) and corresponding power pattern (*central column*) along with the plot the interference suppression function $Q\left(\underline{\theta}, \underline{\phi}\right)$ of the first t on-off sequences (*right column*).
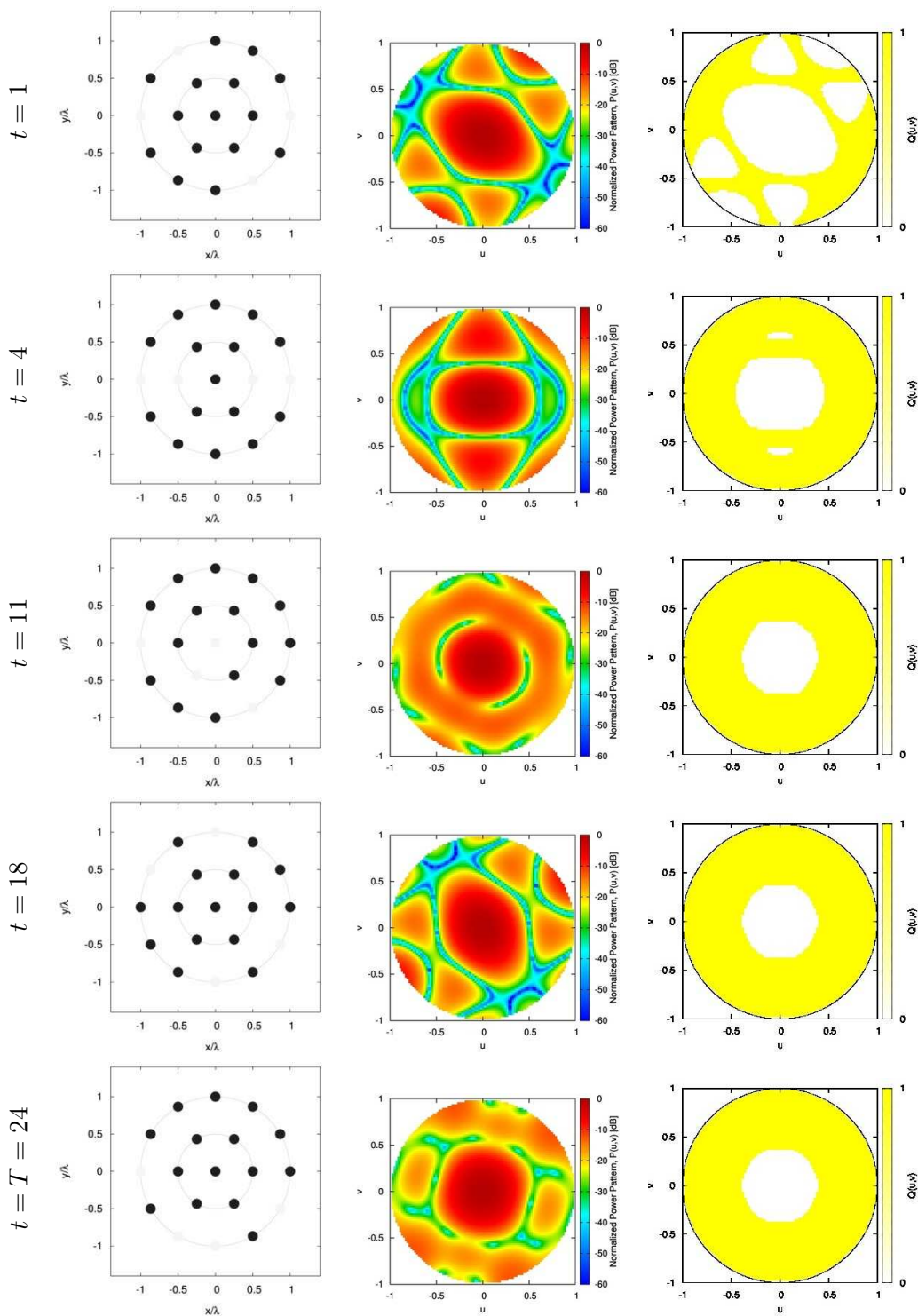
Figure 4. *Example 2* - $[N = 19, d = \frac{\lambda}{2}, N_{on}^{(t)} = 15, SLL_{th} = -30dB]$ - Set of thinning arrays (*left column*) and corresponding power pattern (*central column*) along with the plot of the interference suppression function $Q\left(\underline{\theta}, \underline{\phi}\right)$ of the first t on-off sequences (*right column*).

angular nulling region ($t = 1$ - Fig. 4) satisfy the sidelobe constraint over the 46% of the whole sidelobe region (i.e., almost 30% less than the best configuration of *Example 1*). In order to yield a 96% interference suppression, $t = 11$ sequences are here requested, that is more than five times the number of thinning sequences used in the previous example.

4. Conclusions

A dynamic thinning strategy for the suppression of interferences or jammers impinging on planar ring arrays has been presented and assessed. The array elements, each one controlled with a RF switch, have been dynamically turned on and off according to a set of off-line pre-computed thinning sequences whose radiation patterns present low secondary lobes or nulls along the directions of the undesired signals. From a methodological point of view, the main contribution of this work is the proper extension and customization of the method in [8] to deal with planar architectures as well as its generalization to signals coming from arbitrary directions in the (θ, ϕ) plane. Selected numerical results have been presented to give the interested readers some indications about the effectiveness of the dynamic thinning approach for ring arrays. The numerical analysis has pointed out that it is always possible to synthesize a finite set of thinned sequences generating an interference suppression region extended to the whole sidelobe region, but the size of the thinning set increases when lower sibelobe performances are needed.

References

[1] Mailloux R J 2005 *Phased Array Antenna Handbook* (Norwood MA: Artech House)

[2] Haupt R L 2010 *Antenna Arrays: A Computational Approach* (Hoboken NJ: John Wiley & Sons)

[3] Salucci M, Gottardi G, Anselmi N and Oliveri G 2017 Planar thinned array design by hybrid analytical-stochastic optimization *IET Microw. Antennas Propag.* **11** 1841-1845

[4] Skolnik M I, Sherman J W and Ogg F C 1964 Statistically designed density-tapered arrays *IEEE Trans. Antennas Propag.* **12** 408-417

[5] Haupt R L 1994 Thinned arrays using genetic algorithms *IEEE Trans. Antennas Propag.* **42** 993-999

[6] Quevedo-Teruel O and Rajo-Iglesias E 2006 Ant colony optimization in thinned array synthesis with minimum sidelobe level *IEEE Antennas Wireless Propag. Lett.* **5** 349-352

[7] Nanbo J and Rahmat-Samii Y 2007 Advances in particle swarm optimization for antenna designs: Real-number, binary, single-objective and multiobjective implementations *IEEE Trans. Antennas Propag.* **55** 556-567

[8] Rocca P, Haupt R L and Massa A 2011 Interference suppression in uniform linear arrays through a dynamic thinning strategy *IEEE Trans. Antennas Propag.* **59** 4525-4533

[9] Poli L, Rocca P, Salucci M and Massa A 2013 Reconfigurable thinning for the adaptive control of linear arrays *IEEE Trans. Antennas Propag.* **61** 5068-5077

[10] Brookner E 1991 Antenna array fundamentals - Part 1 in *Practical Phased Array Antenna Systems* (Norwood, MA: Artech House)